Provided for non-commercial research and education use.
Not for reproduction, distribution or commercial use.

(This is a sample cover image for this issue. The actual cover is not yet available at this time.)

This article appeared in a journal published by Elsevier. The attached copy is furnished to the author for internal non-commercial research and education use, including for instruction at the authors institution and sharing with colleagues.

Other uses, including reproduction and distribution, or selling or licensing copies, or posting to personal, institutional or third party websites are prohibited.

In most cases authors are permitted to post their version of the article (e.g. in Word or Tex form) to their personal website or institutional repository. Authors requiring further information regarding Elsevier's archiving and manuscript policies are encouraged to visit:

http://www.elsevier.com/copyright

Author's personal copy

Journal of Alloys and Compounds 558 (2013) 68–72

Contents lists available at SciVerse ScienceDirect

Journal of Alloys and Compounds

journal homepage: www.elsevier.com/locate/jalcom

Mordenite encapsulated with Pt–TiO_2: Characterization and applications for photocatalytic degradation of direct blue dye

R.M. Mohamed [a,b,c,*], E.S. Baeissa [a]

[a] Chemistry Department, Faculty of Science, King Abdulaziz University, P.O. Box 80203, Jeddah 21589, Saudi Arabia
[b] Advanced Materials Department, Central Metallurgical R&D Institute, CMRDI, P.O. Box 87, Helwan 11421, Cairo, Egypt
[c] Center of Excellence in Environmental Studies, King Abdulaziz University, P.O. Box 80216, Jeddah 21589, Saudi Arabia

ARTICLE INFO

Article history:
Received 12 November 2012
Received in revised form 6 January 2013
Accepted 9 January 2013
Available online 24 January 2013

Keywords:
Mordenite zeolite
Ion-exchanged zeolite
Direct blue dye

ABSTRACT

Ti-incorporated mordenite zeolite was prepared by ion-exchange method, while Pt was immobilized on the encapsulated titanium via impregnation method. The produced samples were characterized using X-ray diffraction (XRD), Ultraviolet and visible spectroscopy (UV–Vis), Photoluminescence emission spectra (Pl), Scanning electron microscopy (SEM) and surface area measurement. Furthermore, the catalytic performances of Ti–Pt/mordenite were carried out for degradation of direct blue dye using visible light.

© 2013 Elsevier B.V. All rights reserved.

1. Introduction

Titanium atoms incorporated into the zeolite framework serve as catalytic sites, and thus the content of framework titanium in a zeolite has presented higher activity in performing some catalytic reactions [1–4]. TiO_2 in an anatase phase is the best photocatalyst reported. But, poor adsorption and low surface area properties lead to great limitations in exploiting the photocatalyst. Supporting TiO_2 is commonly reported to be less photoactive due to the interaction of TiO_2 with support during the thermal treatments [5]. Several attempts have been made to improve the photocatalytic efficiency of titania by adding adsorbents like silica, alumina, zeolites, clays, and active carbon [6–12]. This is expected to induce synergism because of the adsorption properties of the adsorbents with respect to organic molecules. Zeolite based photocatalyst is a new work and the work reported so far involved the use of high TiO_2 loadings [13–26].

The potential toxicity of some azo dyes have long been known. The disazo dyes based on benzidine are known to be carcinogenic [27,28]. Several reports on the relation between structure and carcinogenicity of azo dyes have been published [27]. Direct dyes are the compounds able to dye cellulose fibers without the aid of mordant species. Direct dyes constitute about 17% of all dyes used for dyeing textiles and about 30% of the dyes used for dyeing cellulose fibers [29]. A direct blue dye (sodium salt of a sulfonic acid) is an anionic and soluble in water. According to its structure, direct blue dye is a diazo dye based on benzidine. In principle, decoloration is a possible with one or more of the following methods: adsorption, coagulation, biodegradation, chemical degradation, and photodegradation [27]. For adsorption, activated charcoal, silica gel, bauxite, peat, wood, cellulose derivatives, and ion-exchange resins have been used, but these processes are in most cases not economically feasible [27].

The aim of this work is the preparation and catalytic activity of a new photocatalyst for degradation of direct blue dye under visible light, which was synthesized by introducing titania into the pores of mordenite zeolite through ion exchange method while Pt was immobilized on the encapsulated titanium via impregnation method.

2. Experimental details

2.1. Materials

The materials used were silicic acid powder, sodium hydroxide pellets (AR 98%), aluminum sulfate [Merck, $Al_2(SO4)_3{\cdot}16H_2O$], O-phenylenediamine (Merck), and commercial H_2SO_4.

2.2. Preparation of mordenite

The hydrogels of the following oxide molar compositions was arranged for the synthesis of mordenite zeolite: 3.0 Na_2O:0.2 Al_2O_3:6.2 SiO_2:0.2 OPDA:100 H_2O where OPDA is O-phenylenediamine (OPDA) template. A known weight of NaOH was added to silicic acid in calculated amount of H_2O while stirring, followed by heating at 80 °C until a clear solution was obtained. The OPDA was dissolved in a small amount of H_2O followed by heating at 50 °C for 20 min. Subsequently, the solution of OPDA was added to that of sodium silicate while stirring for 15 min.

* Corresponding author at: Chemistry Department, Faculty of Science, King Abdulaziz University, P.O. Box 80203, Jeddah 21589, Saudi Arabia. Tel.: +966 540715648; fax: +966 2 6952292.
E-mail address: redama123@yahoo.com (R.M. Mohamed).

0925-8388/$ - see front matter © 2013 Elsevier B.V. All rights reserved.
http://dx.doi.org/10.1016/j.jallcom.2013.01.041

Author's personal copy

The aluminum sulfate was dissolved in calculated amount of acidified H_2O via addition of 0.05 ml concentrated H_2SO_4. To the latter solution, the combined solution of sodium silicate and OPDA was added followed by stirring for 30 min. The pH of the mixture was adjusted at 11 by using NaOH (0.1 M) and H_2SO_4 (0.1 M) solutions. Finally, the mixture was hydrothermally treated at 160 °C in an oil bath, using stainless steel autoclaves, for 5 days. The autoclaves were removed at the pre-specified time from the oven and quenched immediately with a cold water. The solid product was filtered and washed with distilled water until the pH of the filtrate reached to 8. The products were dried at 110 °C for 24 h then calcined at 550 °C for 5 h in an air oven. This sample was referred as Na-MOR.

2.3. Insertion of TiO_2 nanoparticles into Na-MOR

A conventional ion-exchange method using an aqueous solution of 0.03 M potassium titanooxalate. Then, 1 gm of Na-MOR was added to potassium titanooxalate solution and stirred for 24 h. After the ion-exchange, the zeolite sample was filtered, washed with doubly distilled water to avoid the physically adsorbed titanium species from Pt aggregating on the external surface of the zeolite, then dried for 24 h in an oven at 100 °C. The resulting TiO_2-exchanged Zeolite(Ti–Na-MOR) was calcined at 550 °C for 5 h with a heating rate of 5 °C/min.

2.4. Preparation of Pt/Ti–Na-MOR catalyst

Incipient wetness impregnation was used to introduce different wt.% of Pt onto Ti–Na-MOR. Impregnation of Pt onto Ti–Na-MOR was carried out as follows: H_2PtCl_6 was dissolved in 100 ml of deionized water and stirred. Then a predetermined amount of Ti–Na-MOR was added to H_2PtCl_6 solution and stirred for 24 h at room temperature, evaporating using an oil bath rotary evaporator. The obtained catalyst was dried for 24 h at 100 °C and then calcined at 500 °C for 5 h. The resulting Pt containing Ti–Na-MOR were labeling according to the different wt.% of Pt loading on Ti–Na-MOR such as (0.1% Pt/Ti–Na-MOR, 0.2% Pt/Ti–Na-MOR, 0.3% Pt/Ti–Na-MOR and 0.4% Pt/Ti–Na-MOR).

2.5. Material characterization

X-ray diffraction (XRD) patterns were recorded using a Bruker axis D8 diffractometer with Cu Kα radiation (λ = 1.540 Å) over a 2θ collection range of 4–60°. Surface morphology of the catalyst was examined using a SEM JEOL 5410 (Japan). Nitrogen adsorption and desorption isotherms were measured at −196 °C using a Nova 2000 series Chromatech apparatus. All the samples were degassed at 200 °C for 2 h prior to data collection. Band-gab values of the samples were obtained via UV–Visible diffuse reflectance spectra (UV–Vis-DRS) in air at room temperature in the wavelength range of 200–800 nm using a UV/Vis/NIR spectrophotometer (V-570, JASCO, Japan). Photoluminescence (Pl) emission spectra was recorded with fluorescence spectrophotometer Shimadzu RF-5301.

2.6. Photocatalytic tests

The application of synthesized nanocomposite for the photodegradation of pure DB53 dye was investigated under visible light. The experiments were carried out using a horizontal cylinder annular batch reactor. The photocatalyst was irradiated with a blue fluorescent lamp (150 W) doubly covered with a UV cut filter. The intensity data of UV light is confirmed to be under the detection limit (0.1 mW/cm^2) of a UV radiometer. In a typical experiment, weight of catalyst were suspended into a 300-ml, 100 mg/L pure DB53 dye solution (pH ~ 7). The reaction was carried out isothermally at 25 °C and samples of the reaction mixture were taken at different intervals for a total reaction time of 1 h.

The concentration of the unreacted DB53 dye was analyzed with UV JASCO (V 570). The removal % of DB53 dye was measured by applying the following equation.

$$\%\ \text{Removal efficiency} = (C_o - C)/C_o \times 100 \quad (1)$$

where C_o is the initial concentration of DB53 in solution, C is the remaining concentration in solution after reaction

Before all photocatalytic runs, a fresh solution (300 ml) of DB53 were adjusted to required pH, and the catalyst was suspended. Suspensions were kept in dark and magnetically stirred at 25 °C for 60 min. The results indicate that adsorption efficiency was about 18–20%.

3. Results and discussion

3.1. XRD analysis

Fig. 1 depicts the XRD patterns pertaining to Na-MOR, Ti–Na-MOR, Pt/Ti–Na-MOR showing that the crystallinity of zeolites is found to be unaltered after the ion-exchange process and impregnation method. Actually, the prepared Ti-exchanged zeolite sample and Pt/Ti–Na-MOR don't contain TiO_2 or Pt_2O phase. This indicates

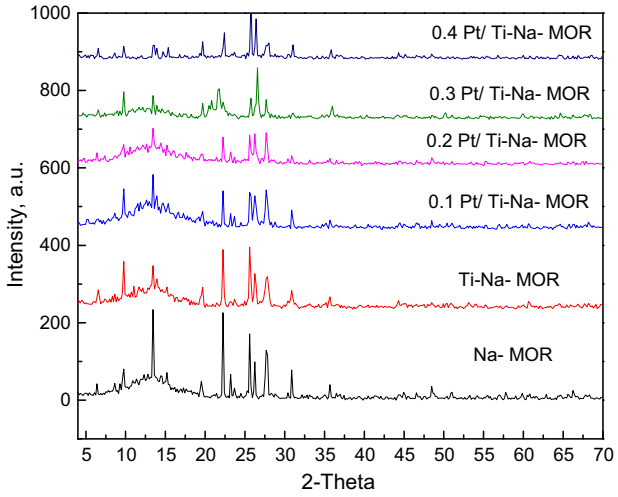

Fig. 1. XRD patterns of Na-MOR, Ti–Na-MOR and Pt/Ti–Na-MOR samples.

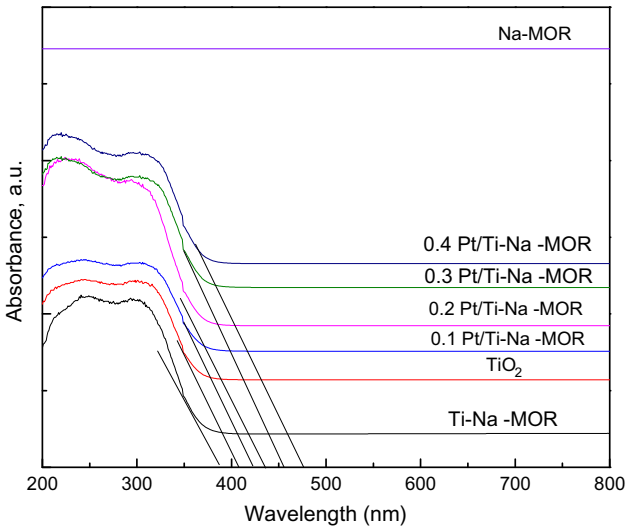

Fig. 2. Diffuse reflectance UV–Vis absorption spectra of Na-MOR, Ti–Na-MOR and Pt/Ti–Na-MOR samples.

Table 1
Relationship of nanocomposite composition and band gap energy.

Sample	Band gap energy (eV)
Na-MOR	–
Ti-MOR	3.2
TiO_2	3.04
0.1% Pt/Ti-MOR	2.90
0.2% Pt/Ti-MOR	2.82
0.3% Pt/Ti-MOR	2.71
0.4% Pt/Ti-MOR	2.60

that the structural damage is negligible during the ion-exchange process and TiO_2 particles residing in the zeolite cavities or channels are too small to be detected by XRD. Also, the absence of peaks for the Pt_2O species was an indication of good distribution of the Pt on the zeolite.

3.2. UV–Vis

The UV–Vis diffuse reflectance spectra of the bulk TiO_2 and titanium-exchanged zeolite catalyst are displayed in Fig. 2. A

Author's personal copy

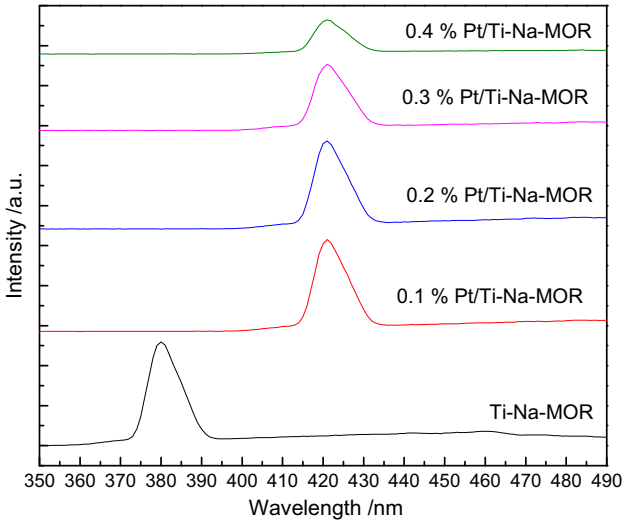

Fig. 3. Pl spectra of Ti–Na-MOR and Pt/Ti–Na-MOR samples.

Table 2
BET surface area of Na-MOR, Ti–Na-MOR and Pt/ Ti–Na-MOR samples.

Sample	S_{BET} (m^2/g)	V_p (cm^3/g)
Na-MOR	410.6	0.330
Ti-Na-MOR	400.3	0.320
0.1% Pt/ Ti–Na-MOR	395.6	0.310
0.2% Pt/ Ti–Na-MOR	390.2	0.308
0.3% Pt/ Ti–Na-MOR	383.6	0.290
0.4% Pt/ Ti–Na-MOR	380.6	0.280

significant blue shift of the spectrum was observed compared with that of a blank titania. Such a shift to the shorter wavelength in the absorption band of titanium oxides can be attributed to the size quantization effect due to the presence of extremely small Ti-oxide particles and/or the bands in the wavelength regions 330–370 nm, and their intensity increases with an increase of Ti content. This result was in agreement with Easwaramoorthi and Natarajan [30]. The sudden fall in the wavelength indicated the presence of optical band gap after the ion exchange of Ti species into the zeolite [31]. These observations proved the success of the ion-exchange process despite of no diffraction peak attributed to TiO_2 observed in the XRD analysis. On the other side, the loading of Pt ions into the Ti–Na-MOR caused a red shift toward higher wavelength from 410 to 476 nm for different loadings of Pt compared to Ti–Na-MOR which had a wavelength of about 388 nm. The direct band gap energy for the bare TiO_2, TiO_2 encapsulated into Na-MOR and Pt/Ti–Na-MOR were calculated from their reflection spectra based on a method suggested by Kumar et al. [32]. The direct band gap energy of the prepared samples are tabulated in Table 1. It is clear that the energy gap decreased with the increase in the Pt ions up to 0.3 wt.%. Also, at higher concentration of Pt ions i.e. 0.4 wt.%, there no significant decrease in the energy band gap was observed. This observation indicated that there was an optimum value for the doping of Pt ion and above this optimum loading value of the optical band gap showed no more direct dependence on the metal ions [33].

3.3. Photoluminescence characteristics

Photoluminescence (Pl) emission spectra have been used to study the transfer of the photogenerated electrons and holes and understand the separation and recombination of photogenerated charge carries. The Pl spectra were detected for the different samples which exited at 300 nm at room temperature and shown in Fig. 3. It is clear that the position of emission of Ti–Na-MOR is different from Pt/Ti–Na-MOR samples and Pl intensity greatly decreased with an increase of the Pt wt.%. Therefore, Pt acts as trapping sites to capture photogenerated electrons from TiO_2 conduction band, separating the photogenerated electron–hole pairs.

3.4. Structural analysis

The BET surface areas of the Na-MOR, Ti–Na-MOR and Pt/Ti–Na-MOR are tabulated in Table 2. A slight reduction in the S_{BET}

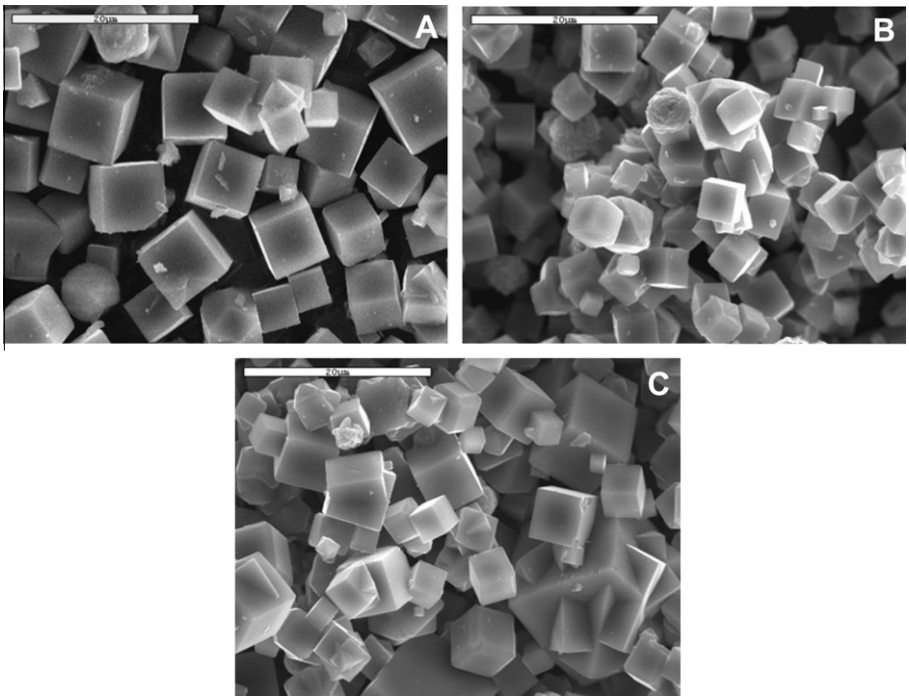

Fig. 4. Surface morphology of (A) Na-MOR, (B) Ti–Na-MOR, (C) 0.3% Pt/Ti–Na-MOR.

Author's personal copy

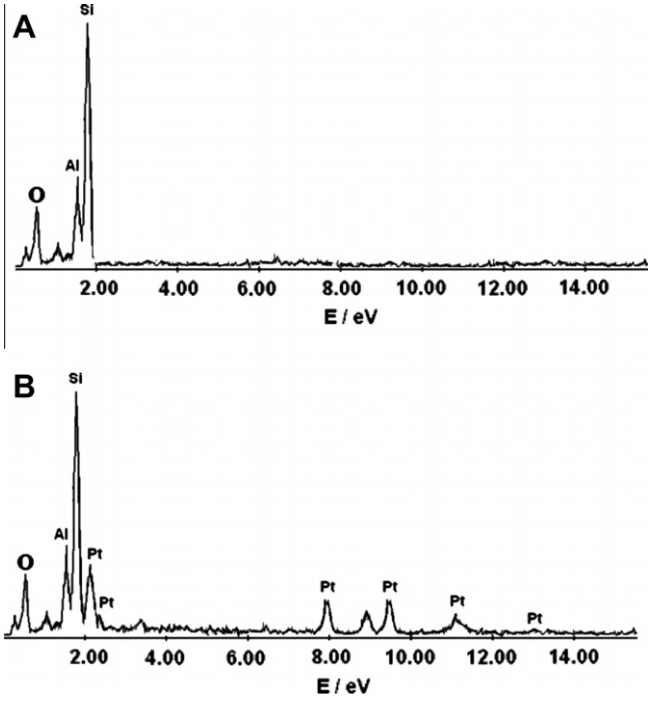

Fig. 5. EDAX analysis results for (A) Ti–Na-MOR and (B) 0.3% Pt/Ti–Na-MOR.

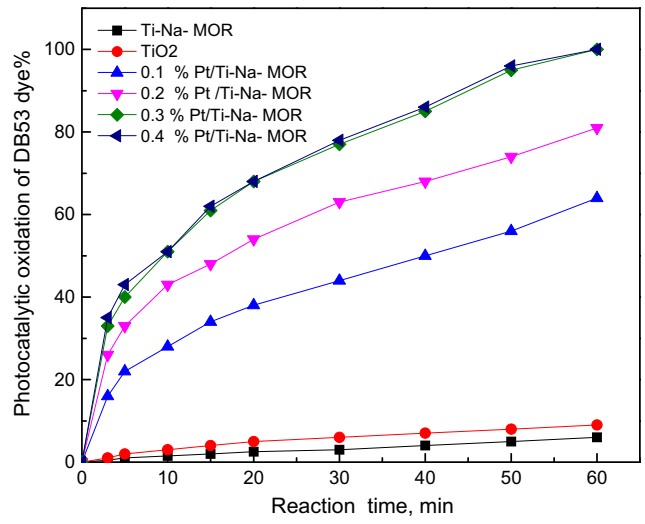

Fig. 6. Photocatalytic degradation of DB53 dye by TiO_2, Ti–Na-MOR and Pt/Ti–Na-MOR samples.

value was observed for Na-MOR from 410.6 m^2/g to 400.3 m^2/g and then reduced to 380.6 m^2/g after 0.4 wt.% Pt was ion exchanged with Ti-mordenite zeolite. This a significant reduction in the surface area after loading of titanium oxide and Pt ions is a good evidence of successful loading of TiO_2 and Pt through the ion-exchange and impregnation method, respectively.

The pore volume of catalyst was found to be slightly decrease from 0.330 cm^3/g for Na-MOR to 0.320 cm^3/g for Ti–Na-MOR. This reduction in pore volume was due to the agglomeration of TiO_2 clusters inside the pores of zeolite after the calcination step.

Additionally, the micrograph structures of the Na-MOR, Ti–Na-MOR and 0.3% Pt/Ti–Na-MOR are seen in Fig. 4. The SEM results were in agreement with the XRD results as there was no major change in the structure. The zeolite was able to keep its crystal

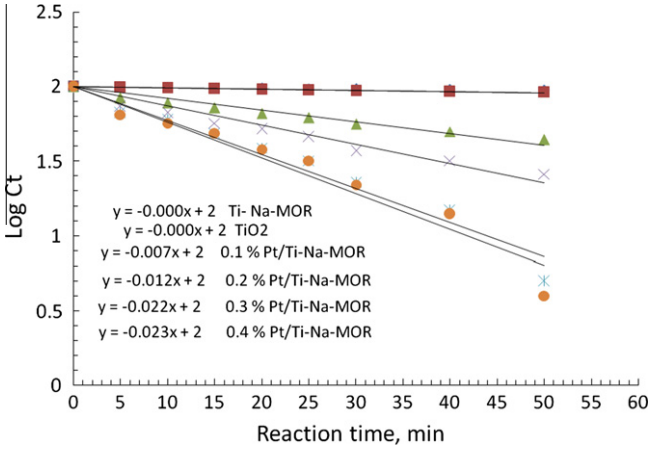

Fig. 7. Rate constant for Na-MOR, TiO_2 and Pt/ Ti–Na-MOR samples.

shape even after the loading of Ti species and Pt ions as was shown in Fig. 4B and C respectively.

On the other hand, the results of EDAX analysis which identify only the surface element of the sample are shown in Fig. 5. The results reveal that there was no specific signal for TiO_2 detected on the surface of the catalyst as shown in Fig. 5A. Therefore, the titanium oxide was deemed to be successfully encapsulated inside the supercages of zeolite through the ion-exchange method. It was in agreement with few earlier studies. For example, Easwaramoorthi and Natarajan [30] did not detect any Ti presented on the external surface of zeolites in the case of TiO_2 encapsulated into zeolite by the ion-exchange method. However, they detected the presence of Ti on the surface of zeolite loaded with TiO_2 that was prepared using sol gel method. Therefore, the preparation method plays an important role in characteristics of the final material. Also, the results reveal that, a small amount of Pt ions was detected to present on the surface of the catalyst as shown in Fig. 5B. So, the results proved that the successful loading of Pt ions through the impregnation method.

3.5. Photocatalytic tests

The prepared samples were tested to degrade of direct blue dye under visible light. The results are summarized in Fig. 6. The results indicate that Ti–Na-MOR and TiO_2 have no photocatalytic activity under visible light duo to their absorbance on UV region. But, an increase of wt.% of Pt from 0.1 to 0.3 wt.% leads to a high direct blue dye removal efficiency from 64% to 100%, respectively. But, above 0.3 wt.% Pt, there no significant effect of wt.% of Pt on the photocatalytic activity.

3.6. Kinetics of direct blue dye

The reaction order with respect to direct blue dye was determined by plotting reaction time *versus* log [direct blue dye] according to the following equation

$$Log[C]_t = -kt + Log[C]_o \quad (2)$$

where $[C]_o$ and $[C]_t$ represent the concentration of the substrate in solution at zero time and t time of illumination respectively, and k represents the apparent rate constant (min^{-1}).

The findings are represented in Fig. 7 and the apparent rate constants are summarized in Table 3. The results show that the reaction followed first order kinetics with respect to direct blue dye and the rate constants were found in the range of 0×10^{-4} to

Author's personal copy

Table 3
Rate constant of reaction kinetic of direct blue dye with Na-MOR, Ti-MOR and Pt/Ti–Na-MOR samples.

Sample	$k \times 10^{-4}$ (min^{-1})
Ti-MOR	0
TiO_2	0
0.1% Pt/Ti-MOR	70
0.2% Pt/Ti-MOR	120
0.3% Pt/Ti-MOR	220
0.4% Pt/Ti-MOR	230

230×10^{-4} min^{-1}. The first order rate equation for direct blue dye is given by: $R = k$ [direct blue dye].

4. Conclusions

The Pt/Ti–Na-MOR photocatalyst was successfully synthesized and it was proven to be a promising catalyst due to its high removal efficiency of the pollutant under visible light. XRD results reveals that a good distribution of the Pt on the zeolite. The UV–Vis analysis proved a red shift was detected after the loading of Pt into the encapsulated titanium-mordenite zeolite. Band gap energy was decreased with the increase in the wt.% of Pt ions up to 0.3 wt.%. At a high concentration of wt of Pt ions i.e. 0.4 wt.%, no significant decrease in the band gap was observed. EDX results reveal that the titanium oxide was deemed to be successfully encapsulated inside the supercages of zeolite through the ion-exchange method and the successful loading of Pt ions through the impregnation method. The maximum degradation efficiency achieved was 100% at 0.3 wt.% Pt/Ti–Na-MOR after 60 min reaction time. The doping of Pt ion into the Ti–Na-MOR was useful in improving the photocatalytic activity. It was due its ability to inhibit the e^-–h^+ recombination produced from the Ti species inside the pores of zeolite.

References

[1] R. Millini, P.E. Massara, G. Perego, G. Bellussi, J. Catal. 137 (1992) 497–503.
[2] A. Thangaraj, R. Kumar, P.S. Mirajkar, P. Ratnasamy, J. Catal. 130 (1991) 1–8.
[3] G. Deo, M.A. Turek, E.I. Wachs, C.R.D. Huybrechts, A.P. Jascobs, Zeolites 13 (1993) 365–373.
[4] E. Astorino, B.J. Peri, J.R. Willey, G. Busca, J. Catal. 157 (1995) 482–500.
[5] O. Legrini, E. Oliveros, A. Braun, Chem. Rev. 93 (1993) 671–698.
[6] F.A. Harraz, O.E. Abdel-Salam, A.A. Mostafa, R.M. Mohamed, M. Hanafy, J. Alloys Comp. 551 (2013) 1–7.
[7] J. Zhao, B. Zhang, Y. Li, L. Yan, S. Wang, J. Alloys Comp. 535 (2012) 21–26.
[8] B. Mazinani, A. Beitollahi, S. Radiman, A. Masrom, S. Ibrahim, J. Javadpour, F.M.D. Jamil, Alloys Comp. 519 (2012) 72–76.
[9] M.A. Ahmed, M.F. Abdel-Messih, Alloys Comp. 509 (2011) 2154–2159.
[10] R.M. Mohamed, I.A. Mkhalid, Alloys Comp. 501 (2011) 301–306.
[11] C. Teh, A. Mohamed, Alloys Comp. 509 (2011) 1648–1660.
[12] A.A. Ismail, I.A. Ibrahim, M.S. Ahmed, R.M. Mohamed, H. El-Shall, J. Photochem. Photobiol. A 163 (2004) 445–451.
[13] B. Sulikowski, J. Klinowski, Appl. Catal. A 84 (1992) 41–153.
[14] C.B. Dartt, C.B. Khouw, H.X. Li, M.E. Davis, Microporous Mater. 2 (1994) 425–437.
[15] S. Zhang, T. Kobayash, Y. Nosaka, N. Fujii, J. Mol. Catal. A: Chem. 106 (1996) 119–123.
[16] S. Zhang, N. Fujii, Y. Nosaka, J. Mol. Catal. A: Chem. 129 (1998) 219–224.
[17] F.S. Zhang, X.W. Guo, X.S. Wang, G. Li, Q. Zhao, X.H. Bao, X.W. Han, L.W. Lin, Mater. Chem. Phys. 60 (1999) 215–220.
[18] G.P. Smirniotis, L. Davydov, Catal. Rev. Sci. Eng. 41 (1999) 43–48.
[19] X. Wang, X. Guo, Catal. Today 51 (1999) 177–186.
[20] M. Kliemkov, A. Nepojko, W. Matz, X. Bao, J. Cryst. Growth 231 (2001) 577–588.
[21] M.R. Prasad, G. Kamalakar, S.J. Kulkarni, V. Raghavan, K.N. Rao, S.S. Prasad, Madhavendra, Catal. Commun. 3 (2002) 399–404.
[22] M. Liu, X. Guo, X. Wang, C. Liang, C. Li, Catal. Today 93–95 (2004) 659–664.
[23] V. Elena, C.L. Robert, L.H. Cooper, J. Phys. Chem. B. 104 (2000) 8679–8684.
[24] X. Yiming, L.H. Cooper, J. Phys. Chem. B. 101 (1997) 3115–3121.
[25] M. Noorjahan, V.D. Kumari, M. Subrahmnyam, P. Boule, Appl. Catal. B 47 (2004) 209–213.
[26] V. Durgakumari, M. Subrahmanyam, K.V. Subba, A. Ratnamala, M. Noorjahan, K. Tanaka, Appl. Catal. A 234 (2002) 155–165.
[27] H. Zollinger, in: H.F. Ebel, C.D. Brenzinger (Eds.), Color Chemistry, first ed., VCH, New York, 1987 (Chapter 16).
[28] W.G. Kuo, Water Res. 26 (1992) 881–886.
[29] N.I. Sax, Cancer Causing Chemical, first ed., VNR, New York, 1981 (DC 9625000).
[30] S. Easwaramoorthi, P. Natarajan, Microporous Mesoporous Mater. 86 (2005) 185–190.
[31] G.P. Joshi, N.S. Saxena, T.P. Sharma, S.C.K. Mishra, Indian J. Pure Appl. Phys. 44 (2006) 786–790.
[32] V. Kumar, S. Kr Sharma, T.P. Sharma, V. Singh, Opt. Mater. 12 (1999) 115–119.
[33] I. Gúth, S. Lukic, J. Optoelectron. Adv. Mater. 3 (2001) 903–908.